

2016

Modeling and Experimental Study of a Heat Pump Water Heater Cycle

Kevin Ruben Deutz

Electricité De France, EDF, France / Institut National des Sciences Appliquées de Lyon, INSA Lyon, kevin-ruben.deutz@edf.fr

Odile Cauret

Electricité De France, EDF, France, odile.cauret@edf.fr

Romuald Rullière

Institut National des Sciences Appliquées de Lyon, INSA Lyon, romuald.rulliere@insa-lyon.fr

Philippe Haberschill

Institut National des Sciences Appliquées de Lyon, INSA Lyon, philippe.haberschill@insa-lyon.fr

Follow this and additional works at: <http://docs.lib.purdue.edu/iracc>

Deutz, Kevin Ruben; Cauret, Odile; Rullière, Romuald; and Haberschill, Philippe, "Modeling and Experimental Study of a Heat Pump Water Heater Cycle" (2016). *International Refrigeration and Air Conditioning Conference*. Paper 1608.
<http://docs.lib.purdue.edu/iracc/1608>

This document has been made available through Purdue e-Pubs, a service of the Purdue University Libraries. Please contact epubs@purdue.edu for additional information.

Complete proceedings may be acquired in print and on CD-ROM directly from the Ray W. Herrick Laboratories at <https://engineering.purdue.edu/Herrick/Events/orderlit.html>

Modeling and Experimental Study of a Heat Pump Water Heater Cycle

Kevin R. Deutz^{1, 2*}, Odile Cauret², Romuald Rulière¹, Philippe Haberschill¹

¹Université de Lyon, CNRS, INSA-Lyon, CETHIL, UMR5008, Villeurbanne
F-69621, France, Université Lyon 1, F-69622, France

²EDF R&D, Energy in Buildings and Territories Department
EDF LAB Les Renardières
Moret sur Loing 77818, France
kevin.ruben-deutz@edf.fr, 0160737312

* Corresponding Author

ABSTRACT

Heat Pump Water Heaters are becoming more and more interesting technologies for efficient sanitary hot water production. The specificities of hot water production compared to the traditional use of heat pumps for space heating are the relatively constant energy needs for different outdoor temperatures and the more rapid dynamics associated with water temperature elevation.

This study focuses on the modeling and performance evaluation of an R134a air to water heat pump water heater with an external mantle heat exchanger. By nature being a thermo-hydraulic kind of system, a heat pump water heater requires both the aspects of fluid mechanics and heat transfer to be covered when modeling the global system composed of the heat pump and the thermal storage tank.

Hence, a detailed thermodynamic model of the heat pump cycle is developed using Modelica covering a description of all the components of the thermodynamic cycle from compressor to evaporator and all the possible operating conditions such as heating and defrosting. This model is associated with a zonal model accounting for the convective behavior patterns of the water observed in the storage tank at different operating conditions and boundary conditions imposed by the heat pump cycle. This dynamic model is compared against experimental data coming from an instrumented system tested in laboratory conditions for different phases such as draw-off, standby and heating. Good precision (<5-10 %) is attained for the heat flow rates, temperatures along the thermodynamic cycle and temperature profiles in the water tank for the different phases tested.

It is shown that the water tank plays an important role in the performances of the system that is very sensitive to the operating conditions such as draw-off flow rate, heat pump operating capacity or thermal losses, that cause mixing and destruction of the thermal stratification and a reduction in the available energy for the end user.

1. INTRODUCTION

Heat Pump Water Heaters (HPWH) have been researched since the 1950s (Hepbasli and Yildiz, 2009). However since the beginning of the 2000's and the emergence of progressively more stringent energy policies, in particular European directives, HPWH have been gaining on market penetration. In France, this is particularly the case where since 2012 a limit has been set on the primary energy consumption of a building. This has put the focus on reducing the heating needs of a building that represent the relative biggest share of the total energy consumption of a building (ADEME, 2014).

In the total energy demand of a building, Domestic Hot Water (DHW) has the particularity to be relatively climate independent (Morrison *et al.*, 2004) and has a seemingly constant relative value of 10 % over the period of 1973 to 2012 of the final energy consumption of a typical French building. The legislative purpose to reduce the overall primary energy consumption implies that in the near future the relative share of the energy demand for hot water in the total energy demand of a building will increase. Within this context electric water heaters (EWH) are becoming less favorable and in most cases will be rejected from a new construction project. HPWH have the advantage of using small heat pump units that being more energy efficient reduce the dependency of hot water production on primary energy compared to EWH.

It was observed that most of the systems actually proposed on the French market consist of a basic vapor compression cycle composed of an expansion valve, an evaporator, a compressor and a condenser that is connected to a water Thermal Storage Tank (TST). Typically three kinds of condenser layouts can be found for the connection between the HP unit and the water TST of the HPWH which are the mantle, immersed and external Heat exchanger (HX). Our investigation relates more specifically to the HPWH system with a mantle type heat exchanger (MHX) that is one of the most commonly proposed systems on the French market.

According to our literature review, numerous studies have been conducted to analyze the performances by means of modeling or experimental testing of HPWH. Most of the studies focused on particular points of the thermodynamic cycle configuration: condenser configuration, refrigerant mixtures or double-stage compression with injection (Kim & Kim, 2014). However, most of these models represent the water TST in a simplified way, by assuming either a fixed temperature in the thermal storage tank or a 1D nodal model. It is believed that in the assessment of the global performance of a HPWH both the heat pump and the TST have to be modeled accurately. Accordingly, the aim of this study is to model a basic thermodynamic cycle with a MHX taking into account both the thermodynamic cycle and the TST's behavior. An experimental study of a HPWH with a MHX, conducted in climatic cells at EDF Lab, is used to evaluate and validate the modeling results.

2. EXPERIMENTAL SET-UP

As to build and validate the model, first an experimental investigation was conducted on one of the most representative HPWH available on the French market. The HPWH with the MHX is a split air source type system with an external unit connected to the water tank through a refrigerant line. The external air unit is composed of the compressor, evaporator and expansion valve whereas the internal unit is composed by a 200 liter tank with wrap-around MHX condenser (Figure 1). The general specifications of the HPWH are given in Table 1. In Figure 1 a general schematic representation of the tank and its instrumentation is given. The tank was instrumented with internal PT100 1/10DIN type temperature sensors disposed vertically at an approximately equidistant interval of 17cm inside the TST. The Heat Pump was instrumented with PT100 temperature sensors all along the height of the MHX condenser surface, temperature sensors at the entrance and the outlet both on the air and fluid side of the evaporator as well as surface temperatures over its copper coils. Electric power was measured with a Yokogawa watt meter with a precision of 0.2 %, energy delivered from the tank during draw-offs was measured with a Endress+Hauser mass flow meter with a precision of 0.5 % and PT100 1/10DIN temperature sensors disposed at the inlet and outlet of the tank.

Table 1: General data concerning the heat pump and the TST

Heat Pump Specifications	
Total power (W)	2800
Heat Pump Maximum electric power (W)	1000
Electric auxiliary heater power (W)	1800
Refrigerant type/mass (kg)	R134a / 1.1
Tank specifications	
Volume (l)	200
Dimensions HxWxD (m)	1.37x0.53x0.6
Upper height of the MHX (m)	0.13
Lower height of the MHX (m)	0.73
Number of coils	52
MHX internal diameter (m)	0.0085
Width of the MHX wall (m)	0.003
Width of the tank isolation wall – extremities (m)	0.035-0.02
Width of the tank isolation over the MHX (m)	0.02

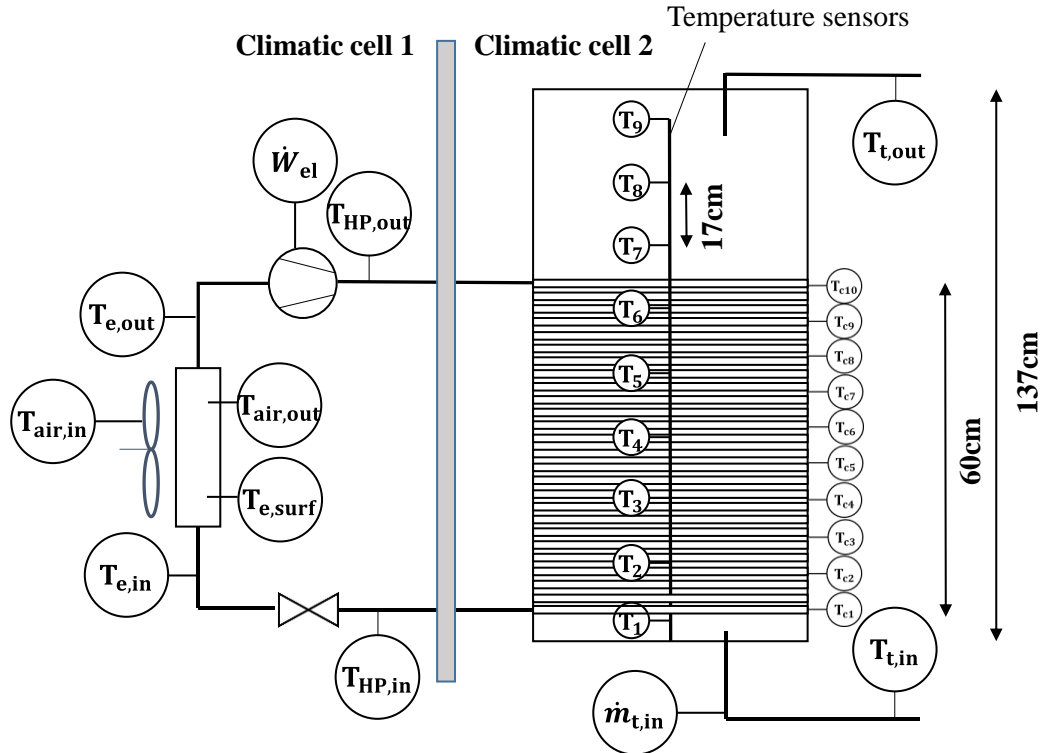


Figure 1: Experimental set-up and instrumentation of the HPWH with MHX

The HPWH is tested by means of two climatic controlled cells (Figure 1), one simulating an external air condition with an imposed temperature and humidity and another simulating an interior air. The operating conditions of the system during the experimental tests are resumed in Table 2.

3. MODELING THE HEAT PUMP

As a thermo-hydraulic kind of system, a HPWH is composed of two major components which are the water Thermal Storage Tank (TST) and the Heat Pump (HP) unit. This means that for the purpose of modeling, both parts' relative contribution in the energy transformation from electricity fed to the compressor to the final end-user's DHW demand have to be taken into account.

The model was developed under Modelica language which allows an acausal object oriented kind of modeling. The numerical solving procedure was done with Dymola© developed by Dassault Systèmes AB (Dassault Systèmes AB, 2014) which has predefined explicit and implicit integrated solvers. The numerical solver chosen was the Radau implicit scheme with a tolerance of 10^{-6} .

The heat pump unit is modeled with the TIL© thermal component library developed by TLK-GmbH and the thermal properties along the cycle are calculated with TILmedia © (Schulze et al., 2015). The heat pump model developed is of semi-empirical gray-box nature. As such the heat exchangers are based on energy and mass conservation with empirical correlations used for the heat transfer and pressure drop calculation. On the other hand the compressor model is based on constructor data.

Table 2: Operating conditions during the experimental investigation

Ambient temperature, T_a (°C)	20
Tank temperature setpoint, T_{set} (°C)	55
External air temperature (°C)	7
Incoming water temperature, $T_{t,in}$ (°C)	10
Initial water temperature, $T_{t,init}$ (°C)	10
Air relative humidity ratio, H (%)	87

3.1 Modeling the compressor and the expansion valve

The compressor is a small capacity rotary type compressor of 13 cm³. The only outputs of interest for thermodynamic cycle modeling are the discharge temperature, the mass flow rate and the electric power consumed (Li, 2013). All three were calculated using empirical fitted relations for the volumetric efficiency, the isentropic efficiency and the global efficiency of the compressor. For volumetric efficiency, it is common to fit a linear decreasing law as function of compression ratio. However it was observed from constructor data that there was a strong dependency on the evaporating temperature. Consequently, the best fitting function was found to be:

$$\eta_v = a_0 - a_1 \left(\frac{P_c}{P_e} \right)^{1/k} + a_2 T_e + a_3 T_e^2 \quad (1)$$

For the isentropic efficiency, a dependency was found with the evaporating and condensing temperatures, as:

$$\eta_{is} = b_0 + b_1 \left(\frac{P_c}{P_e} \right) + b_2 \left(\frac{P_c}{P_e} \right)^2 + b_3 T_e + b_4 T_c \quad (2)$$

The global efficiency allows to determine the electric power from the isentropic power as:

$$\dot{W}_{el} = \frac{\dot{W}_{is}}{\eta_g} \quad (3)$$

Where the global efficiency was calculated according to constructor data as proposed by Ghoubalia et al. (2014):

$$\eta_g = c_0 + c_1 \left(\frac{P_c}{P_e} \right) + c_2 \left(\frac{P_c}{P_e} \right)^2 + c_3 \left(\frac{P_c}{P_e} \right)^3 + c_4 \left(\frac{P_c}{P_e} \right)^4 + c_5 T_e + c_6 T_c \quad (4)$$

The electronic expansion valve is assumed to be isenthalpic and the mass flow rate is calculated as:

$$\dot{m}_{EEV} = A_{eff} \sqrt{2 \rho_{c,out} (P_c - P_e)} \quad (5)$$

3.2 Modeling the heat exchangers

The MHX condenser is assumed to behave like a finite length horizontal tube. The modeling approach adopted by TIL-TLK (Schulze et al., 2015) consists in discretizing in n cells following the finite volume approach. The heat transfer correlations used for one phase heat transfer are Gnielinski's for Reynolds numbers ranging from 2300 to 10000 and Dittus Boelter's for Reynolds numbers superior to 10000. Two phase heat transfer coefficient's are determined using Shah's correlation. The pressure drop is calculated using Konakov's correlation for smooth pipes.

The fin and tube evaporator is modeled using finite volumes method. Same approach as for the condenser has been chosen for one phase heat transfer. Two phase convective and nucleate heat transfer is calculated using Shah's correlation for low Froude numbers inferior to 0.04 and Chen's correlation for higher Froude numbers.

4. MODELING THE THERMAL STORAGE TANK

The main aim for the water TST is to shift heat generation from the actual use. This allows to use smaller dimensioned heat pump units that heat the water in the TST during periods when the DHW needs are low. Naturally when water is heated inside a tank, a density gradient is generated and a temperature stratification appears following Archimedes' principle. In this way the buoyancy forces drive the hot water to the upper part of the tank and the colder water stays in the bottom part. In terms of energy, this stratification effect allows to maintain the useful energy in the top part of the tank where it will finally be drained.

Different phenomena have been found in literature that can play a role in the performance of the thermal storage tank but the main causes of stratification disturbance or destratification are respectively the inlet water jets that mix with the water in the TST and the thermal heat losses to the ambient. Different types of modeling strategies exist with different grades of precision. On the one hand 3D CFD models are computationally intensive but precise and on the other hand one can make the hypothesis of a stirred volume with one global temperature and discard stratification completely. Experimentally, it was observed that the fluid's thermal and dynamic behavior was dependent on the operating conditions that define different boundary conditions for the TST system. As such, a hybrid modeling approach was opted for, specific to the heating, standby heat losses and draw-off periods.

4.1 Modeling the heat-up

For the heat-up phase, the zonal approach proposed by Kenjo et al. (2003) was chosen. This model is based on the hypothesis of a thermal and inertial boundary layer forming along the tank wall when heated by the MHX, consequently forming a convective Rayleigh-Bénard type of cell as shown in Figure 2. For simulation, 10 isothermal cells were used in the vertical direction and 7 cells in the horizontal direction, taking into account the mantle HX, the tank wall, the boundary layers and the central region of the tank. An axial symmetry was used to simplify the model.

The upflowing mass flow rate in the boundary layer was determined by using Bejan's (2013) temperature and velocity profiles for turbulent flow and integration along the cross sectional surface of the boundary layer. For an element i,j of the boundary layer, this results in:

$$\dot{m}_{bl,i,j} = 0.098 \alpha \rho Pr^{\frac{1}{15}} \left[\frac{Ra_{i,j}}{1 + 0.494 Pr^{\frac{2}{3}}} \right]^{\frac{2}{5}} p \quad (6)$$

Kenjo et al.'s (2003) model assumes a mantle-heat exchanger positioned along the total height of the tank. Consequently, the entrainment flow entering the boundary layer depicted by the horizontal arrows in Figure 2 would be « egoistically positive » all over the height of the tank. It was observed that this leads to numerical inconsistencies with a MHX covering only a given height of the tank, leading to « negative flows » outcoming the boundary layer in the parts of the tank with a negative temperature gradient between the wall temperature and the initial water temperature. As such, the following condition was added to the numerical solving procedure:

$$\dot{m}_{i,j} = \begin{cases} \dot{m}_{bl,i,j} & Ra_{i,j} > Ra_{i-1,j} \\ \dot{m}_{i-1,j} & Ra_{i,j} \leq Ra_{i-1,j} \end{cases} \quad (7)$$

The idea is that once the buoyancy forces of the superior layer are inferior to the buoyancy forces of the inferior layer then there is no more entrainment flow. In other words, this hypothesis assumes that the buoyancy flow generated by the hot wall has sufficient inertia to reach the upper part of the tank without major velocity drop.

This initial model proposed by Kenjo et al. (2003) related to heating phase only assuming an initial uniform water tank. However it was observed experimentally that for an initial stratified case, the natural convection cell had a varying extent according to time. This allowed us to make the hypothesis of a specific dynamic behavior associated with the convection cell. More precisely, it was seen that the upward boundary flow would only reach the levels of similar temperature levels and density levels. As such, an additional flow/no-flow condition was added to the model:

$$\dot{m}_{i,j} = \begin{cases} \dot{m}_{bl,i,j} & T_{i,j} > T_{i+1,j+1} \\ 0 & T_{i,j} \leq T_{i+1,j+1} \end{cases} \quad (8)$$

Having the entrained mass flow rates allows to close the system for a i cell and to calculate all the other mass flows from the j cells surrounding based on steady state assumption and the flow pattern assumption given in Figure 2 as:

$$\sum_j \dot{m}_{i,j} = 0 \quad (9)$$

The heat transfer for a given cell i and the j cells (north, south, east and west) surrounding can be calculated as:

$$c_{v,i} V_i \frac{dT_i}{dt} = - \sum_j [(U_{i,j} A_{i,j} (T_i - T_j) + \dot{m}_{i,j} c_p (T_i - T_j))] \quad (10)$$

Where $U_{i,j}$ represents the overall heat transfer coefficient with the neighboring cells that can be either conductive and/or convective. In case of a heating period Shah (2000)'s heat transfer correlation is used:

$$Nu(z) = (4.501 - 3.103 \frac{D_t}{H_t}) \left(\frac{g \beta (T_p(z) - T_\infty) z^4}{\nu \alpha H_t} \right)^{0.19} \quad (11)$$

$$h_{conv}(z) = \frac{Nu(z) z}{k} \quad (12)$$

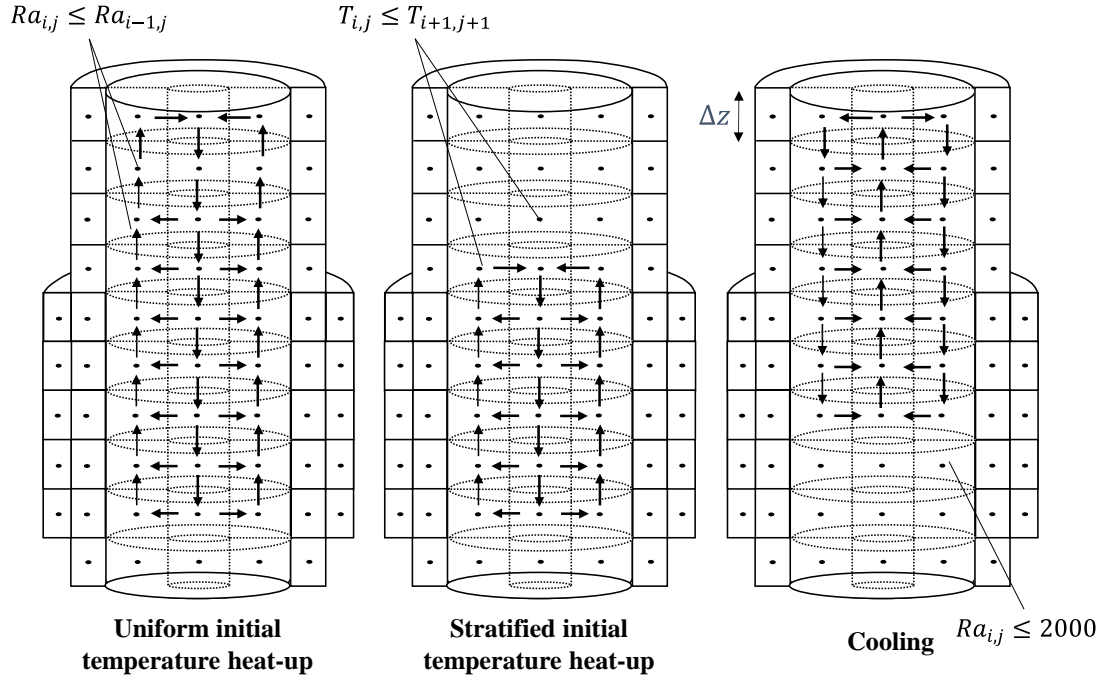


Figure 2: Different flow patterns in the MHX thermal storage tank according to operating conditions

4.2 Modeling the standby periods

Oliveski (2013) observed with CFD that a descending boundary layer flow forms along the water tank wall during standby-periods. As suggested by Kenjo et al. (2003), the zonal model would hence fit very well too, this time not with an upward flow but downwards calculated in the same ways as eq. (6). This was however yet not confronted to experimental data.

It was suggested by Kenjo et al. (2003) that this flow pattern would exist all along the tank wall. However the CFD performed by Oliveski (2013) and Furbo (2012) let us believe that this is not always the case. Their results seem to demonstrate that the boundary layer reduces until extinction with time. This reduction of the mass flow rate is directly taken into account by the temperature gradient appearing in the Rayleigh number that progressively reduces while reaching equilibrium. For the case of total extinction of the boundary layer, a lower limit has to be taken into account where the fluid's viscous forces are greater than the buoyancy forces. According to Kaminski and Jensen (2011) this happens when the Rayleigh number is below 2000. An extra condition was hence added to the flow resolution as:

$$\dot{m}_{i,j} = \begin{cases} -\dot{m}_{bl,i,j}, & Ra_{i,j} > 2000 \\ 0, & Ra_{i,j} \leq 2000 \end{cases} \quad (13)$$

The convective heat transfer during cool down phases was obtained using Oliveski (2013)'s correlation as:

$$\overline{Nu} = 1.86 A_c^{1.11} \hat{U}^{0.174} (Pr Ra^*)^{0.155} \quad (14)$$

4.3 Modeling draw-offs

It was observed experimentally that two types of flow region exist in the tank when drawing-off water at a given flow rate. First a piston type flow seemed to exist in the upper part of the tank. This piston type flow is a general assumption taken by a lot of authors from literature. Another region seemed to exist in the bottom part of the tank closest to the tank inlet. This region seemed to be subject to intense mixing with the incoming cold water flow and its extent in the tank seemed to increase with time. A lot of parameters affect the dynamics of this mixing region such as tank and (cold water) inlet design, incoming water flow rate, incoming water temperature and tank temperature.

For this study, it is assumed that mixing occurs at a fixed height from the inlet and that the piston type flow appears all over the height of the tank. As such, the energy balance for a horizontal layer i in the vertical direction with the j cells surrounding can be formulated as:

$$c_{v,i} V_i \frac{dT_i}{dt} = \begin{cases} - \sum_j [U_{i,j} A_{i,j} (T_i - T_j)] + \frac{\dot{m}_{DHW} c_p (T_{i_{mix}} - T_{in})}{i_{mix}}, & i \leq i_{mix} \\ - \sum_j [U_{i,j} A_{i,j} (T_i - T_j)] + \dot{m}_{DHW} c_p (T_{i-1} - T_i), & i > i_{mix} \end{cases} \quad (15)$$

5. RESULTS AND DISCUSSION

5.1 Validation of the TST model

The validation of the tank model is done upon three different temperature levels in the tank. This allows to validate the behavior of the tank profile according to the height of the tank.

In figure 3, the TST model is confronted to experimental data for a heating period (from 10 °C to 55 °C) followed by a standby phase at 20 °C ambient temperature. It can be seen that water in the tank reaches its temperature set point after approximately 7 hours. For the bottom layer of the tank it can be seen that a heating lag exists between the heating start-up phase and the temperature elevation in this region. This heating lag is due to the time necessary to the tank walls to heat up, the boundary layer to form and to transport sufficient energy after successive heat up of the higher zones.

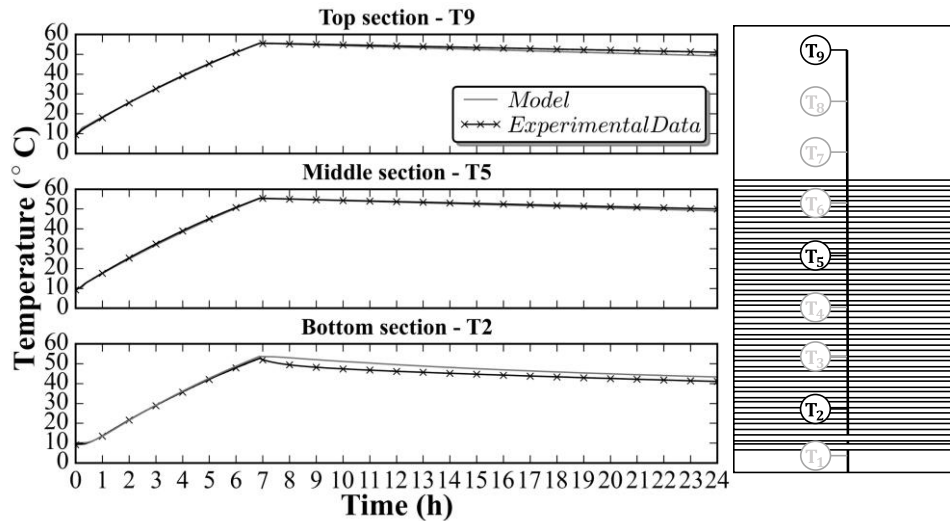


Figure 3: Heating from uniform temperature of 10 °C to 55 °C followed by a standby-period in a 20 °C ambient temperature environment with 10 °C external temperature

Also it is interesting to point out that the zonal model predicts the temperatures along the whole height of the tank with a good precision. In the standby-period from hour 7 to 24, the model predicts with a good accuracy the temperatures in the high and middle region of the tank. In the bottom section, although the tendency seems to be similar, there exists a persisting error of 2 K. Those errors can be related both to the boundary layer mass flow correlation and to the numerical precision of the grid that were used in this study.

In figure 4, successive heat-up and draw-off phases are presented. At a draw-off flow rate of 720 l/h an acceptable precision is found at the different heights of the tank. The stratified reheating phase that follows seems also to be well predicted. However for a 120 l/h draw-off flow rate there seems to be an imprecision of the model in the higher regions of the tank. This can be related to the precision of the numerical grid employed. Indeed it is assumed that 10 horizontally mixed regions exist, subject to the plug flow and mixing regime. In reality, a cold water front rises cooling infinitesimally small layers of the tank in a successive manner. As such, the temperature predicted by the model relates more to an average temperature of a plurality of infinitesimal layers different from the sensors that measure the real temperature of one given infinitesimal layer.

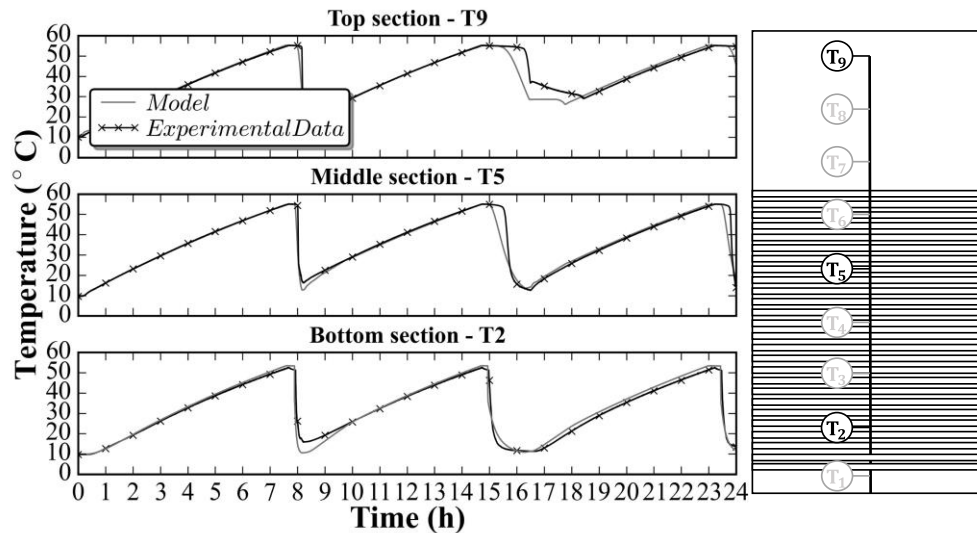


Figure 4: A heat-up phase at 7 °C external temperature, followed by a draw-off at 720 l/h, reheat and a draw-off at 120 l/h with reheat

The mixing model employed assumes a fixed height. However in figure 4 it can be seen that a deviation exists in the lower layer temperature predictions for the 720l/h draw-off where for 120l/h this deviation is smaller. Consequently, a possible improvement for the mixing model would be to correlate the mixing layer height with the influencing parameters such as draw-off flow-rate and water inlet temperature.

5.2 Validation of the Heat Pump model

For the heat pump validation both temperatures around the cycle and electric power consumed by the compressor measured experimentally (Figure 1) represent important characteristics to validate. Figure 5 shows the validation of the model in the condenser and evaporator parts. For the condenser, the model is validated in the superheat, condensation and subcooling regions (on the refrigerant side). The condensation temperature rises both in the model and experiment with the elevation of the water to 55 °C. For the evaporator, the model is validated on the air and refrigerant sides, with a satisfying prediction. However, a small error of 1.7 K exists for the refrigerant inlet temperature prediction. This can be related to the connecting tubes and collector that were not taken into account in the model.

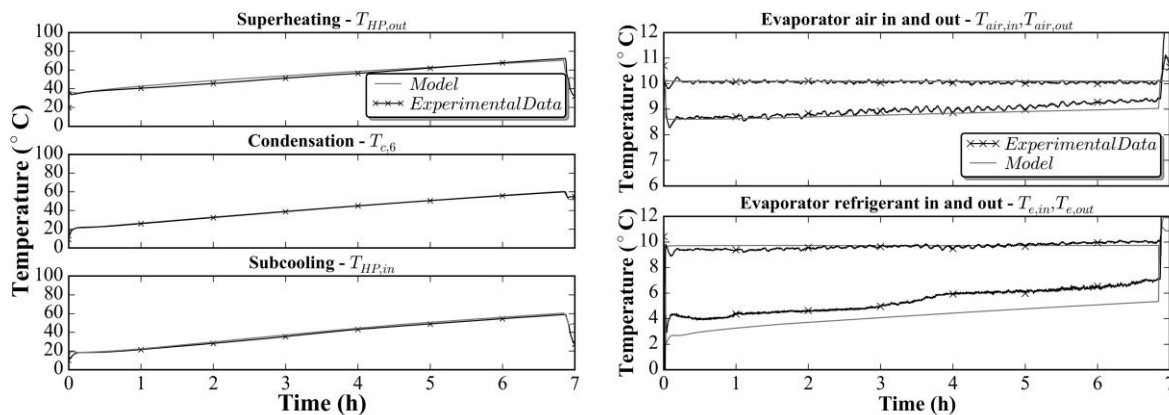


Figure 5: Condenser and evaporator boundary validation for a heating phase at 10 °C external temperature

In figure 6, the power consumed by the compressor is confronted at different evaporator air inlet temperatures. The compressor model seems to present acceptable precisions with small deviations at the end of the heat-up phase. This can be explained by the precision of the empirical mapping employed, variable according to the condensing and evaporating temperature regions.

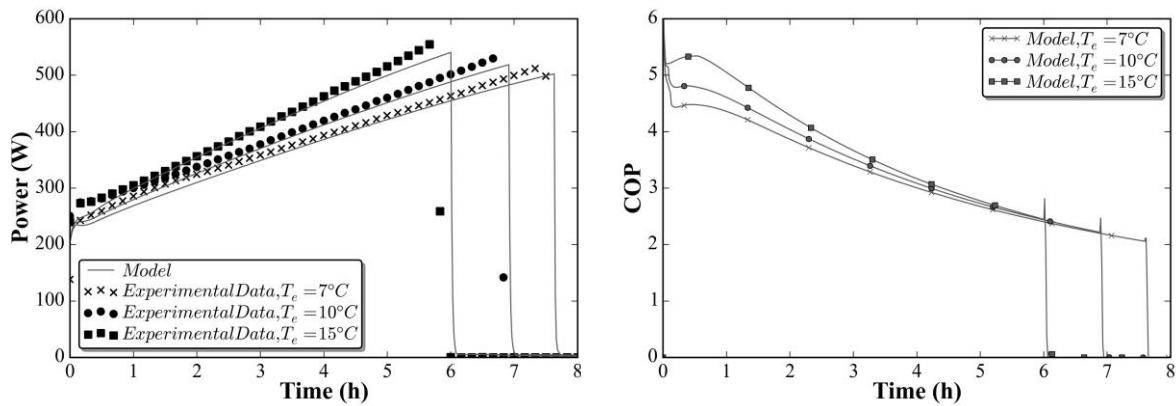


Figure 6: Predicted and experimental power at different evaporator temperature levels and predicted COP

The Coefficient of Performance (COP) could not be confronted to the model as there was no measure done yet on the refrigerant mass flow rate in the heat pump unit. The prediction presented in figure 6 seems however to be coherent with physical considerations. In the start-up phase the heat pump has a lower COP due to the thermal inertia of the heat pump cycle. Then an optimum is reached once the cycle is in steady-state and has a low tank water temperature hence low condensing pressure. Then the COP decreases with the increase of the condensation temperature following the increase of water temperature all along the heat-up phase.

6. CONCLUSIONS

A general thermodynamic model was built for the purpose of simulating a heat pump connected to a water thermal storage tank. A fluid mechanics based zonal model from literature was used for the tank assuming boundary layer flow during heat-up and cooling periods. The boundary layer flow's region of influence was determined according to physics based criterions. A semi-empirical approach was used to model the heat pump with empirical data for the compressor and general heat transfer correlations for the discretized heat exchangers. These two combined approaches allow to simulate the behavior of a Heat Pump Water Heater with a mantle heat exchanger in a numerical efficient, modular and precise way. Such a model can be used for the purpose of optimization and yearly simulations as it allows both low simulation time and high precision in the results.

NOMENCLATURE

A	Surface	(m^2)
A_c	Modified aspect ratio	(m^2)
c_v	Specific volumetric heat capacity	($\text{J}/^\circ\text{C}/\text{m}^3$)
c_p	Specific heat capacity at constant pressure	($\text{J}/^\circ\text{C}/\text{kg}$)
D	Diameter	(m)
g	Gravity	(m/s^2)
H	Height	(m)
h_{conv}	Convective heat transfer coefficient	($\text{W}/\text{m}^2/^\circ\text{C}$)
k	Conductive heat transfer coefficient	($\text{W}/\text{m}/^\circ\text{C}$)
\dot{m}	Mass flow rate	(kg/s)
Nu	Local Nusselt Number	(—)
P	Pressure	(Pa)
Pr	Prandtl number	(—)
Ra	Rayleigh number	(—)
Ra^*	Modified Rayleigh number	(—)
T	Temperature	($^\circ\text{C}$)
U	Overall heat transfer coefficient	($\text{W}/\text{m}^2/^\circ\text{C}$)
\bar{U}	Dimensionless overall heat transfer coefficient	(—)

V	Tank volume	(m ³)
\dot{W}	Power	(W)
z	Vertical axe coordinate	(m)
Δz	Vertical layer height	(m)
η	Efficiency	(–)
ρ	Density	(kg/m ³)
α	Thermal diffusivity	(m ² /s)
p	Tank perimeter	(m)
β	Thermal expansion coefficient	(/°C)
ν	Cinematic Viscosity	(m ² /s)
Subscript		
bl	Boundary layer	
c	Condensation	
e	Evaporation	
EEV	Electronic Expansion Valve	
eff	Effective	
el	Electric	
g	Global	
i, j	Increments	
is	Isentropic	
v	Volumetric	

REFERENCES

- ADEME. (2014). *Climat, air et énergie*. French environment and energy management agency.
- Bejan, A. (2013). *Convection Heat Transfer*. New Jersey: Wiley.
- Dassault Systèmes AB. (2014). *Dynamic Modeling Laboratory User Manual Volume 1 Version 17*.
- Ghoubalia, R., Byrne, P., Miriel, J., & Bazantay, F. (2014). Simulation study of a heat pump for simultaneous heating and cooling coupled to buildings. *Energy and Buildings* 72, 141-149.
- Hepbasli, A., & Yildiz, K. (2009). A review of heat pump water heating systems. *Renewable and Sustainable Energy Reviews* 13, 1211-1229.
- Jianhua Fan, S. F. (2012). Buoyancy driven flow in a hot water tank due to standby heat loss. *Solar Energy* 86, 3438-3449.
- Kaminski, D., & Jensen, M. (2011). *Introduction to Thermal and Fluids Engineering, Updated Edition*. Wiley.
- Kenjo, L. (2003). Etude Du Comportement Thermique D'un Chauffe-Eau Solaire A Faible Debit. Université de Nice-Sophia Antipolis: Rapport de thèse.
- Kim, D. H., & Kim, M. (2014). The effect of water temperature lift on the performance of cascade heat pump system. *Applied Thermal Engineering* 67, pp. 273-282.
- Li, W. (2013). Simplified steady-state modeling for variable speed compressor. *Applied Thermal Engineering* , 50, 318-326.
- Morrison, G., Anderson, T., & Behnia, M. (2004). Seasonal performance rating of heat pump water heaters. *Solar Energy* 76, 147-152.
- Navarro-Esbrí, J. (2014). Shell-and-tube evaporator model performance with different two-phase flow heat transfer correlations. Experimental analysis using R134a and R1234yf. *Applied Thermal Engineering*, 62, 80-89.
- Oliveski, R. D. (2013). Correlation for the cooling process of vertical storage tanks under natural convection for high Prandtl number. *International Journal of Heat and Mass Transfer*, 57, 293-298.
- Schulze, C., Raabe, G., Tegethoff, J., & Köhler, J. (2015). Transient evaluation of a city bus air conditioning system with R-445A as drop-in – From the molecules to the system. *International Journal of Thermal Sciences*, 355-361.